

Broadband and wide-angle reflective polarization converter based on metasurface at microwave frequencies

Linbo Zhang¹ · Peiheng Zhou¹ · Haiyan Chen¹ · Haipeng Lu¹ · Jianliang Xie¹ · Longjiang Deng¹

Received: 14 April 2015 / Accepted: 8 July 2015 / Published online: 17 July 2015
© Springer-Verlag Berlin Heidelberg 2015

Abstract We propose to realize a broadband and wide-angle reflective polarization converter in microwave regions. The proposed converter can convert a linearly polarized (LP) wave to its cross-polarized wave at three resonant frequencies. It can also convert the LP wave to a circularly polarized wave at other two resonant frequencies. Furthermore, the proposed converter can achieve broad bandwidth with incident angle up to 45°. The simulated and measured results are in agreement in the entire frequency regions, and the bandwidth of polarization conversion over 75 % can be obtained from 7.6 to 15.5 GHz under normal incidence and from 7.8 to 13.0 GHz under incident angle of 45°. The surface current distributions of the proposed converter are discussed to analyze the physical mechanism. The converter tolerance to wide angle of incidence and the broad bandwidth could be useful in the range of applications in the microwave regions.

1 Introduction

Metamaterials (MMs), as a rapidly developing cutting-edge research field, have drawn much attention due to their unprecedented electromagnetic (EM) properties discovered [1]. Many special functional devices based on these exotic properties can be developed, such as perfect absorbers [2],

high-impedance surfaces (HIS) [3], and EM cloaks [4]. Polarization conveys valuable information for EM signal processing [5, 6]. It has been widely used in many EM applications, including microwave communications, manufacture of antennas, and astronavigation. Conventional polarization converters employing the Brewster effects or birefringence [7] usually require quite long propagation distance to obtain the phase accumulation. Expanding the limited bandwidth of the conventional polarization converters requires complex designs using multilayered films or Fresnel rhombs [8]. Therefore, it is important to develop simple broadband polarization control devices with small thickness.

Recently, MMs have been used to manipulate EM properties by chiral and anisotropic MMs [9, 10]. Many MMs structures such as metal split-ring resonators (SRRs) present polarization conversion [11, 12]. However, the disadvantage of these polarization converters based on MMs is its narrow operating bandwidth, which impedes their application in practice [13, 14]. Many methods and designs have been proposed to extend the polarization conversion bandwidth. Feng et al. [15] proposed a reflective polarization rotator based on HIS, which can generate multiorder plasmon resonances. Despite its relatively small thickness, the rotator has only 1.5 GHz bandwidth. Huang et al. [16] proposed a multiband reflective polarization converter using U-shaped MMs, which can convert the linearly polarized (LP) wave to its cross-polarized wave. However, the polarization conversion only occurs at three resonant frequencies. Grady et al. [6] have designed a linear polarization converter operating in reflection using metallo-dielectric MMs in terahertz frequency region, and the bandwidth could be extended in some degree with a relative thinner thickness, which gives us some new ideas to design broadband

✉ Linbo Zhang
zlbyeah0806@126.com

¹ National Engineering Research Center of Electromagnetic Radiation Control Materials, State Key Laboratory of Electronic Thin Film and Integrated Devices, University of Electronic Science and Technology of China, Shahe Campus: No. 4, Section 2, North Jianshe Road, Chengdu 610054, Sichuan, People's Republic of China

polarizer with small thickness in the microwave frequency regions.

In this paper, a broadband and wide-angle polarization converter can be realized based on metasurface in microwave regions. A triple-band, cross-reflective polarization conversion can be obtained when it is illuminated by a LP wave. Meanwhile, the LP wave can be converted to a circularly polarized (CP) wave at other two resonant frequencies. Moreover, the broadband properties can be sustained at the incident angle up to 45° . The measured polarization conversion bandwidth of reflectance over 0.75 is achieved from 7.6 to 15.5 GHz under normal incidence and from 7.8 to 13.0 GHz under incident angle of 45° . Compared with the previous designs, the proposed reflective polarization converter has simple geometry and broad bandwidth and tolerance to wide incident angles.

2 Design and simulation

Figure 1a shows the photograph of the proposed converter used in the experiment and the schematic diagram of one unit cell. The converter can rotate polarization state completely to its orthogonal counterpart. The structure consists of three layers, with resonant metallic patterns arranged on the top layer periodically. The middle layer is dielectric substrate, and the bottom layer is a full metallic sheet, as shown in Fig. 1b, c. Figure 1b gives the front view of individual unit cell. The geometrical parameters of the converter are as follows: $p = 9.0$ mm, $l_1 = 5.5$ mm, $w_1 = 1.5$ mm, $l_2 = 1.5$ mm, $w_2 = 0.25$ mm, $l_3 = 3.0$ mm, $w_3 = 0.5$ mm, and $t = 3.0$ mm.

The numerical simulation is carried out to analyze the reflection characteristics of the polarization converter with a commercial program, CST MICROWAVE STUDIO

2013. In the simulations, the periodic boundary conditions are used in unit cell and the metal material is copper (with a conductivity of 5.8×10^7 S/m), and the substrate is FR4 (with a dielectric constant 4.3 and a loss tangent 0.025).

To better understand the polarization conversion of the designed structure, we suppose the incident wave is y-polarized, $\vec{E}^{\text{in}} = \hat{e}_y^{\text{in}} e^{i(-\vec{k}_{\text{in}} \cdot \vec{r} + \omega t)}$, and the reflected wave can be written as $\vec{E}^r = (r_{yy} \hat{e}_y^r + r_{xy} \hat{e}_x^r) e^{i(-\vec{k}_r \cdot \vec{r} + \omega t)}$, where \hat{e}_y^{in} , \hat{e}_y^r , \hat{e}_x^r are the unit **E** vectors in different directions, \vec{k}_{in} , \vec{k}_r are the wave vectors, r_{yy} and r_{xy} represent the reflection coefficient of y-to-y and y-to-x polarization conversion, respectively. We define a polarization conversion ratio (PCR) as $\text{PCR} = r_{xy}^2 / (r_{xy}^2 + r_{yy}^2)$. And $r_{xy}/r_{yy} = |r_{xy}/r_{yy}| e^{i\Delta\varphi_{xy}}$, $\Delta\varphi_{xy}$ is the phase difference between the y and x components of the reflected EM waves. $\Delta\varphi_{xy}$ can take arbitrary values with $[-180^\circ, 180^\circ]$ depending on the frequency, indicating that all possible polarization states are realizable for the reflected waves. The linearly polarized wave converts to its cross-polarization wave as $\Delta\varphi_{xy} = 0^\circ$ (or $\Delta\varphi_{xy} = \pm 180^\circ$). The linearly polarized wave converts to a CP wave as $|r_{xy}| = |r_{yy}|$ and $\Delta\varphi_{xy} = \pm 90^\circ$. Others are elliptically polarized waves. Also, η is the angle between its polarization direction and the y-axis, and then $\eta = \tan^{-1}(|E_{xy}|/|E_{yy}|)$.

3 Experiment results and discussion

3.1 Sample fabrication and measurement results

Figure 1a shows the photograph of the fabricated broadband polarization converter, which was fabricated into a 20 by 20 unit sample (180×180 mm²) by the conventional printed circuit board (PCB) process with the sample structural parameter as the simulated model. A double-side

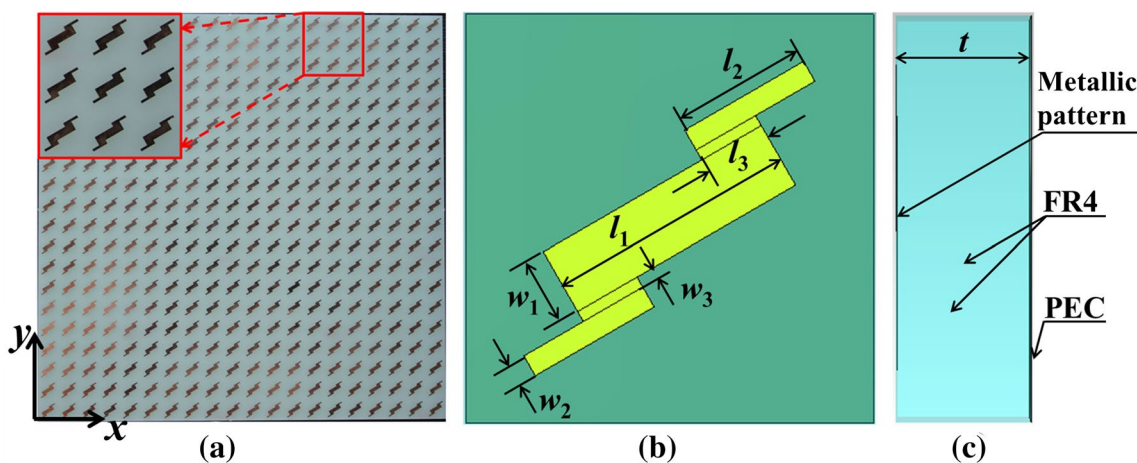


Fig. 1 The unit cell of the proposed structure: **a** a part of photography of the measured sample, **b** front, and **c** lateral view of the unit cell

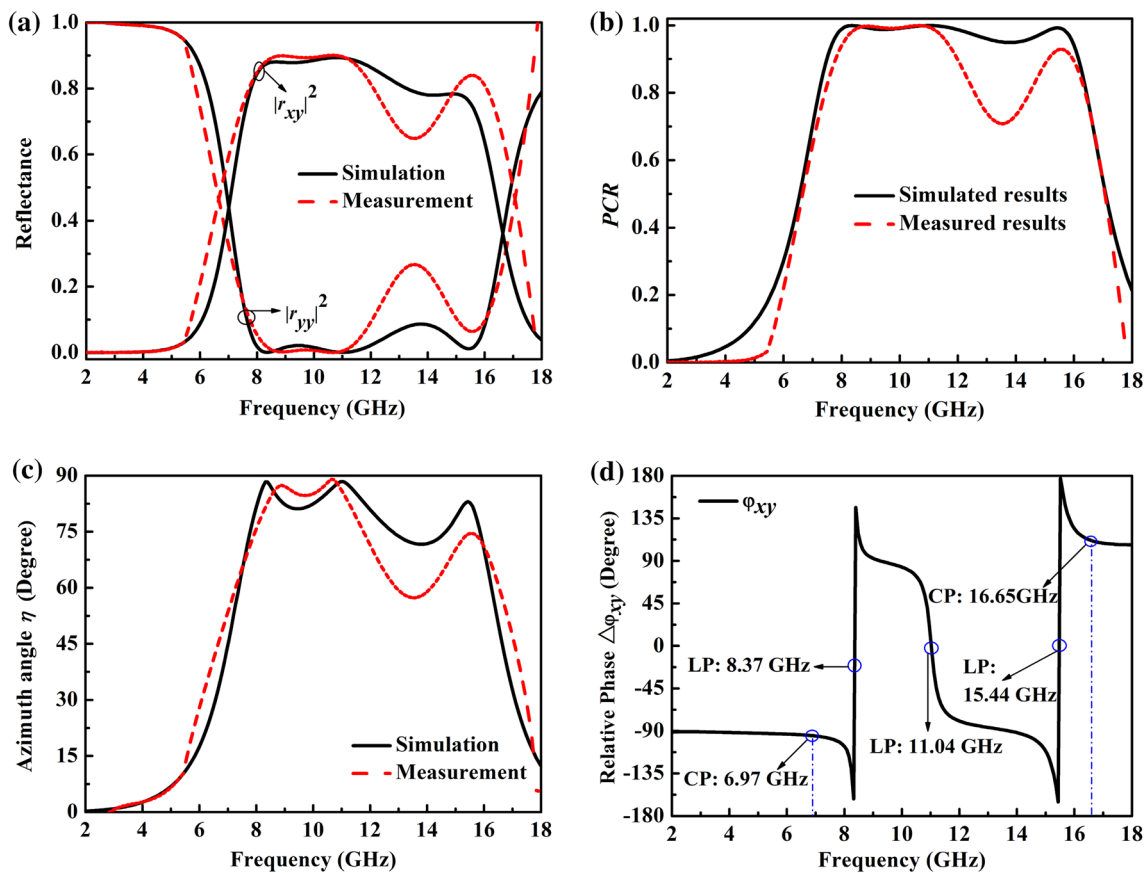


Fig. 2 Simulated and measured results of LP conversion pattern under y -polarized incident wave. **a** Reflectance of $|r_{xy}|^2$ and $|r_{yy}|^2$. **b** PCR and polarization azimuth rotation angle η , **d** simulated relative phase $\Delta\phi_{xy}$ versus frequency between r_{xy} and r_{yy}

copper-cladding PCB board is etched with resonator patterns on the one side, while the copper cladding is kept on the other side.

The simulated and measured results of LP incident waves are shown in Fig. 2a. The measured reflectance is very similar to the simulated ones except that there is a difference at high frequencies, due to the major reason of the finite number of unit cells in the experiments. From Fig. 2a, it can be obtained clearly that the bandwidth of simulated reflectance $|r_{xy}|^2$ is over 0.75 in 7.6–15.5 GHz, and $|r_{xy}|^2$ is 0.88, 0.89, and 0.76 at three neighboring frequencies of 8.37, 11.06, and 15.44 GHz. The measured reflection $|r_{xy}|^2$ is 0.89, 0.90, and 0.72 at three frequencies of 9.0, 10.7, and 15.6 GHz, respectively. PCR at three frequencies are 1.0, 1.0, and 95.7 % for simulations and 1.0, 1.0, and 92.3 % for measurement, respectively, as shown in Fig. 2b. At the three frequencies, PCR nearly achieves 1.0, which means nearly all energy of y -polarized incident wave is converted to x -polarized ones. Figure 2c employs the polarization azimuth rotation angle η to describe the angle between the major polarization axis and y -axis. It is more intuitive that the polarization conversion changes versus frequency.

We can see that the values of η for measurement are 87.3°, 89.0°, and 74.5° at 9.0, 10.7, and 15.6 GHz for y -polarized incident wave. It is further confirmed that the y -polarized wave is almost converted to x -polarized wave at the three frequencies. The simulated relative phase difference of $\Delta\phi_{xy}$ under y -polarized illumination is shown in Fig. 2d. It can be seen that the value of $\Delta\phi_{xy}$ is close to the vicinity of zero or $\pm 180^\circ$ at three frequencies of 8.37, 11.06, and 15.44 GHz, respectively, which means the polarization states are converted. We name the three frequencies as resonant frequencies. At the frequency of 6.97 GHz, the $|r_{xy}|^2 = |r_{yy}|^2 = 0.44$, and $\Delta\phi_{xy} = 90^\circ$, indicating a pure CP wave. At the frequency of 16.65 GHz, $|r_{xy}|^2 = |r_{yy}|^2 = 0.36$, and $\Delta\phi_{xy} = 111^\circ$ little larger than 90° , indicating a non-pure CP wave. At other frequencies, elliptically polarized waves are obtained.

3.2 Surface current distribution for normal incidence

From the simulated and measured results, it can be seen that the converter has a broadband property. This is due to the structure's multiple resonances. At the three resonance

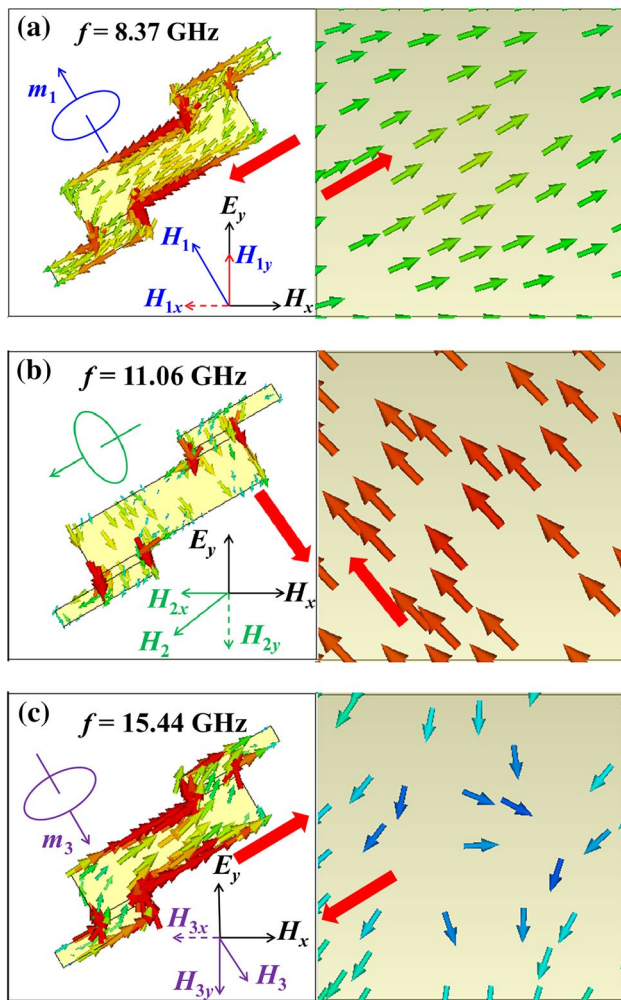


Fig. 3 Surface current distributions of the proposed converter. **a**, **b**, and **c** represent surface current distributions of the front (left) and bottom layer (right) at resonant frequencies of 8.64, 10.88, and 15.44 GHz, respectively

frequencies, the function of the converter can be anisotropic high-impedance surface (HIS) [17, 18]. The reflected waves along x - and y -axis have different reflection phases, respectively, and then the polarization state of reflected waves is converted.

To understand the physical mechanism of the polarization converter, the surface current distributions for the top layer and the bottom metal ground at the resonant frequencies are presented. Figure 3 shows the instantaneous induced surface current distributions of the front and back layers in the converter at resonant frequencies of 8.37, 11.06, and 15.44 GHz, respectively. When the incident wave is y -polarized, the antiparallel current at the top and bottom metallic layers excites at 8.37 GHz, which results in the magnetic dipole moments m_1 (blue color). The y component (H_{1y}) of the induced magnetic field H_1 paralleled to the incident electric field E_y ; then, the cross-coupling

between the incident electric field E_y and H_{1y} of the induced magnetic field leads to a cross-polarization with an y -to- x polarization conversion [6]. The similar physical mechanism occurs at resonant frequencies of 11.06 and 15.44 GHz, depicted in Fig. 3b, c. The cross-coupling effect between incident electric field E_y and H_{2y} , E_y and H_{3y} , leads to the y -to- x polarization conversion, respectively. In summary, the x components (H_{1x} , H_{2x} , and H_{3x}) of the induced magnetic field are perpendicular to the incident field E_y , which cannot excite the cross-polarization due to the same direction of the incident magnetic field. The induced magnetic field (H_{1y} , H_{2y} , and H_{3y}) is parallel to the incident electric field E_y and thus can induce an electronic field (E_x) perpendicular to the incident electric field (E_y). The induced electric field E_x results in the polarization conversion.

3.3 Polarization conversion dependent on incident angle

As is indicated by the above discussions, further numerical simulations and experiments revealed that the broadband and high-efficient conversion properties are sustained over a wide incident angle (θ) range. Figure 4a, b illustrates the simulated reflectance of $|r_{xy}|^2$ and $|r_{yy}|^2$ under different θ , respectively. It is shown that the polarization conversion efficiency can be sustained as incident angle increases. Even though the bandwidth is decreased, the polarization conversion bandwidth over 75 % can be achieved from 7.8 to 13.0 GHz at incident angle of 45° . For the oblique incident measurement, horn antennas are rotated keeping the rotator at fixed position. The incident angle is kept for 45° . Figure 4c shows the measured data of $|r_{xy}|^2$ and $|r_{yy}|^2$. Here, the converter exhibits a broadband polarization conversion over 75 % from 8.2 to 13.6 GHz. However, there is a minor shift for the measured resonant frequencies, owing to the fabrication precision as well as the dielectric board material whose actual dielectric constant is slightly different from the value used in the simulations. Meanwhile, the edge diffraction of the finite unit cells for oblique incident measurement is the major factor that affects experimental precision.

3.4 Polarization state dependent on thickness t

To further broaden the application range of interest, we investigate the effect of the thickness on polarization states at desired frequencies. In Fig. 5a, the results reveal insensitivity to the variation of thickness, suggesting good tolerance to the broadband property. In Fig. 5b, it is obtained that the variation of thickness does not affect the polarization states at resonant frequencies of nearly 8.37 and 15.44 GHz. However, between the above two resonant frequencies, the LP wave can be excited, and the resonant

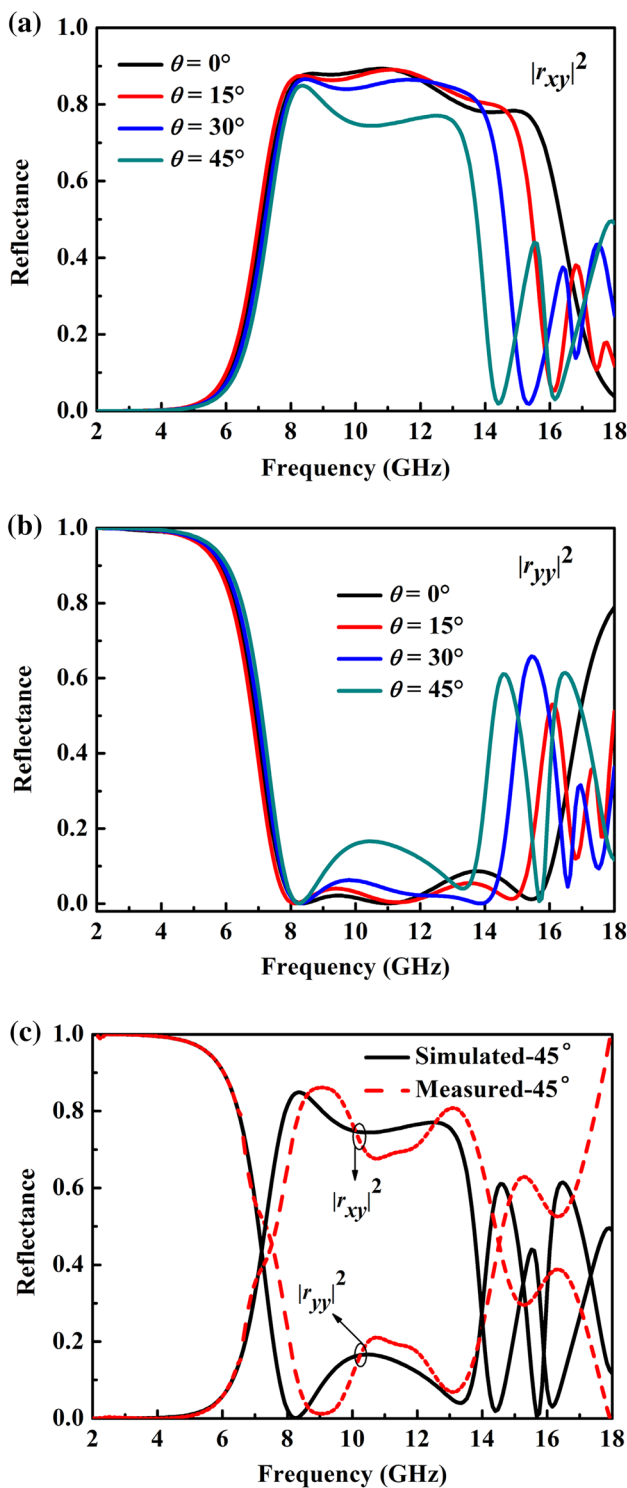


Fig. 4 Simulated results of **a** $|r_{xy}|^2$ and **b** $|r_{yy}|^2$ under different incident angle from 0° to 45° . **c** Simulated and measured magnitudes of $|r_{xy}|^2$ and $|r_{yy}|^2$ for incident angle of 45°

frequency corresponding to the linear polarization state shifts toward low frequencies as thickness increases. Hence, it is demonstrated that we can tweak the structural

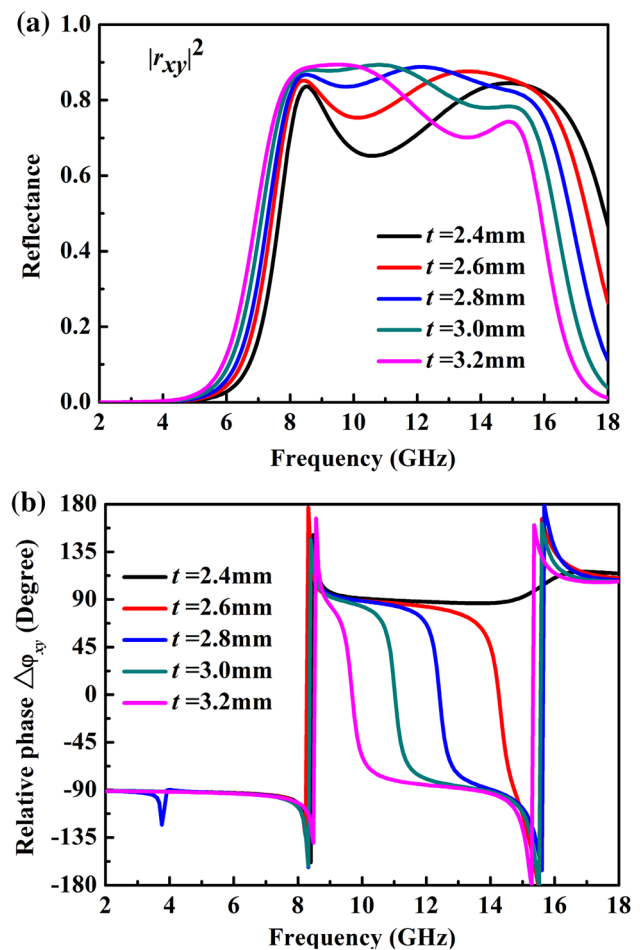


Fig. 5 Simulated results of the converter: **a** simulated reflectance of $|r_{xy}|^2$ and **b** simulated relative phase between r_{xy} and r_{yy} versus frequency with different thickness t

thickness at the unit cell level to customize requirements at desired frequencies, thus enhancing the practicality of the proposed converter.

In the end, the improvement in high-efficient and broadband polarization conversion based on metasurface is a commonly designed method. However, most designed converter mainly analyzes the polarization conversion under the unchangeable frequencies. The polarization states of the proposed converter here can be changed easily by adjusting the geometrical parameters. Therefore, we will be able to further study the active polarization control based on the proposed converter.

4 Conclusion

In conclusion, we have numerically and experimentally proposed a broadband and wide-angle reflective polarization converter. The converter can convert a LP wave to its

cross-polarized wave at three neighboring frequencies. It can also convert the LP wave to a CP wave at other two resonant frequencies. The polarization states can be easily adjusted by tweaking the structural thickness. Moreover, the proposed converter can achieve broad bandwidth at incident angle up to 45° . And the measured polarization conversion is over 75 % from 7.6 to 15.5 GHz under normal incidence and from 7.8 to 13.0 GHz under incident angle up to 45° . The physical mechanism is illustrated by the surface current distributions. The converter tolerance to wide angles of incidence, the adjustment of polarization conversion at desired frequencies, and the broadband property could be widespread applications in the microwave regions.

Acknowledgments The authors are grateful to the supports from the National Natural Science Foundation of China under Grant Nos. 51025208 and 61001026, the Program for Changjiang Scholars and Innovative Research Team in University, the Fundamental Research Funds under Grant No. ZYGX2013J029, and the Open Foundation of National Engineering Research Center of Electromagnetic Radiation Control Materials under Grant ZYGX2013K001-5.

References

1. D.R. Smith, J.B. Pendry, M.C.K. Wiltshire, *Science* **305**, 788 (2004)
2. N.I. Landy, S. Sajuyigbe, J.J. Mock, D.R. Smith, W.J. Padilla, *Phys. Rev. Lett.* **100**, 207402 (2008)
3. D. Sievenpiper, L. Zhang, R.F.J. Broas, N.G. Alexopolous, E. Yabonovitch, *I.E.E.E. Trans, Micro. Theory Tech.* **47**, 2059 (1999)
4. D. Schurig, J.J. Mock, B.J. Justice, S.A. Cummer, J.B. Pendry, A.F. Starr, D.R. Smith, *Science* **314**, 977 (2006)
5. J.D. Jackson, *Classical Electrodynamics*, 3rd edn. (Wiley, New York, 1999)
6. N.K. Grady, J.E. Heyes, D.R. Chowdhury, Y. Zeng, M.T. Reiten, A.K. Azad, A.J. Taylor, D.A.R. Dalvit, H.T. Chen, *Science* **340**, 1304 (2013)
7. M. Born, E. Wolf, *Principle of Optics*, 6th edn. (Pergamon, Oxford, 1980)
8. R.A. Shelby, D.R. Smith, S. Schultz, *Science* **292**, 77 (2001)
9. A.V. Rogacheva, V.A. Fedotov, A.S. Schwanecke, N.I. Zheludev, *Phys. Rev. Lett.* **97**, 177401 (2006)
10. J.Y. Chin, M. Lu, T.J. Cui, *Appl. Phys. Lett.* **93**, 251903 (2008)
11. Z. Wei, Y. Cao, Y. Fan, X. Yu, H. Li, *Appl. Phys. Lett.* **99**, 221907 (2011)
12. Z. Li, R. Zhao, T. Koschny, M. Kafesaki, K.B. Alici, E. Colak, H. Caglayan, E. Ozbay, C.M. Soukoulis, *Appl. Phys. Lett.* **97**, 081901 (2010)
13. J. Zhou, D.R. Chowdhury, R. Zhao, A.K. Azad, H.-T. Chen, C.M. Soukoulis, A.J. Taylor, J.F. O'Hara, *Phys. Rev. B* **86**, 035448 (2012)
14. N. Kanda, K. Konishi, M. Kuwata-Gonokami, *Opt. Express* **15**, 11117 (2007)
15. M. Feng, J. Wang, H. Ma, W. Mo, H. Ye, S. Qu, *J. Appl. Phys.* **114**, 074508 (2013)
16. X. Huang, D. Yang, H. Yang, *J. Appl. Phys.* **115**, 103505 (2014)
17. H. Chen, J. Wang, H. Ma, S. Qu, Z. Xu, A. Zhang, M. Yan, Y. Li, *J. Appl. Phys.* **115**, 154504 (2014)
18. L. Zhang, P. Zhou, H. Chen, H. Lu, J. Xie, L. Deng, *IEEE Trans. Antennas and Wireless Propag. Lett.* **14**, 1157 (2015)